CHEMISTRY OF MATERIALS
Article

Chem. Mater. **2010,** *22,* 2261–2267 2261
DOI:10.1021/cm902610f

In vitro and In vivo Optical Imaging Using Water-Dispersible, Noncytotoxic, Luminescent, Silica-Coated Quantum Rods

Rajiv Kumar, Hong Ding, Rui Hu, Ken-Tye Yong, Indrajit Roy, Earl J Bergey, and Paras N Prasad*

Institute for Lasers Photonics and Biophotonics, State Univerity of New York at Buffalo, Buffalo, New York 14260

Received August 24, 2009. Revised Manuscript Received January 7, 2010

A facile method for synthesis of monodisperse, biocompatible, silica coated CdSe/CdS/ZnS quantum rods (QRs) and their use as probes for in vitro and in vivo optical bioimaging is presented. The silica coating procedure involves condensation-polymerization of the precursor tetraethylorthosilicate (TEOS) over QRs encapsulated within the reverse micellar core of Igepal CO-520/cyclohexane microemulsion. The silica-coated QRs have been characterized by TEM, DLS, and photoluminescence spectroscopy. The silica shell thickness has also been shown to be tuned by varying the ratio of TEOS and QRs. Confocal bioimaging of different cell lines (Panc 1 and RAW), treated with silica coated QRs, has shown a robust uptake of the nanoparticles, without the need of specific targeting molecules. To evaluate the cytotoxicity of the nanoparticles, MTS assay has been carried out over a period of 48 h. In vivo imaging of subcutaneously xenografted tumor-bearing mice, following direct intratumoral injection of the nanoparticles, have shown fluorescence from the tumor within 10 min of injection. This study suggests that these silica-coated QRs can be potentially used for long-term targeted imaging studies in vitro and in vivo.

Introduction

Recent progress in optical fluorescence imaging, with development of various fluorescent probes, offers enhanced imaging sensitivity and high spatial resolution.[1−3] Optical imaging with fluorescent probes has a wide range of applications ranging from in vitro cellular tracking to early diagnosis of cancer in vivo. The synthesis, surface chemistry, conjugation of colloidal semiconductor nanocrystals (quantum dots/rods), and their core/shell structures for ultrasensitive in vitro and in vivo imaging have seen major recent advances.[4−9] The use of these nanocrystals offers many advantages over the conventional organic dye molecules that include high photobleaching threshold, good chemical stability, and readily tunable spectral properties.[10,11] One-dimensional semiconductor nanostructures, such as quantum rods and wires, hence remained among the intensive research topics because of their potential applications in targeted bioimaging.[12−15] CdSe-based quantum rods (QRs) have been extensively studied because of their unique optical and electronic properties, sharp emission band with broad excitation, and strong resistance to photobleaching.[16,17] Also, emission color control is achievable by controlling the rod dimension.[18] Additionally, polarized emission was detected for rods related with their cylindrical symmetry and this degree of polarized emission is dependent on the aspect ratio of the nanocrystals.[19] QRs are brighter single-molecule probes as compared to their counterpart quantum dots. These unique characteristics of QRs as biological markers may provide an avenue for further improvements in ultrasensitive imaging strategies. The use of QRs for biomedical research began very recently because of the advancement of solution-phase synthesis techniques. For the last two years, our group has been actively engaged

*Corresponding author. E-mail: pnprasad@buffalo.edu.

(1) Michaelis, J.; Hettich, C.; Mlynek, J.; Sandoghdar, V. *Nat. Med.* **2000**, *405*, 586.
(2) Prasad, P. N. *Introduction to Biophotonics*; Wiley-Interscience: New York, 2003.
(3) Bruchez, M. Jr.; Moronne, M.; Gin, P.; Weiss, S.; Alivisatos, A. P. *Science* **1998**, *281*, 2013.
(4) Chan, W. C. W.; Maxwell, D. J.; Gao, X. H.; Bailey, R. E.; Han, M. Y.; Nie, S. M. *Curr. Opin. Biotechnol.* **2002**, *13*, 40.
(5) Yong, K. T.; Hu, R.; Roy, I.; Ding, H.; Vathy, L. A.; Bergey, E. J.; Mizuma, M.; Maitra, A.; Prasad, P. N. *ACS Appl. Mater. Interfaces* **2009**, *1*, 710.
(6) Fu, A.; Gu, W.; Boussert, B.; Koski, K.; Gerion, D.; Manna, L.; Gros, M. L.; Larabell, C. A.; Alivisatos, A. P. *Nano Lett.* **2007**, *7*, 179.
(7) Gao, X.; Dave, S. R. *Adv. Exp. Med. Biol.* **2007**, *620*, 57.
(8) Jiang, W.; Papa, E.; Fischer, H.; Mardyani, S.; Chan, W. C. *Trends Biotechnol.* **2004**, *22*, 607.
(9) Voura, E. B.; Jaiswal, J. K.; Mattoussi, H.; Simon, S. M. *Nat. Med.* **2004**, *10*, 993.
(10) Amieson, T.; Bakhshi, R.; Petrova, D.; Pocock, R.; Imani, M.; Seifalian, A. M. *Biomaterials* **2007**, *28*, 4717.
(11) Romero, M. J.; vandeLagemaat, J.; Mora-Sero, I.; Rumbles, G.; Al-Jassim, M. M. *Nano Lett.* **2006**, *6*, 2833.
(12) Zimnitsky, D.; Xu, J.; Lin, Z.; Tsukruk, V. V. *Nanotechnology* **2008**, *19*, 215606.
(13) Burda, C.; Chen, X.; Narayanan, R.; El-Sayed, M. A. *Chem. Rev.* **2005**, *105*, 1025.
(14) Han, T.-T.; Fu, Y.; Wu, J.; Yue, Y.; Dai, N. *J. Phys. D: Appl. Phys.* **2008**, *41*, 115104.
(15) Li, X.; Embden, J.; Chon, J. W. M.; Gu, M. *Appl. Phys. Lett.* **2009**, *94*, 103117.
(16) Htoon, H.; Hollingworth, J. A.; Malko, A. V.; Dickerson, R.; Klimov, V. I. *Appl. Phys. Lett.* **2003**, *82*, 4776.
(17) Shabaev, A.; Efros, L. *Nano Lett.* **2004**, *4*, 1821.
(18) Li, L.; Hu, J.; Yang, W.; Alivisatos, A. P. *Nano Lett.* **2001**, *1*, 349.
(19) Hu, J.; Li, L.; Yang, W.; Manna, L.; Wang, L.; Alivisatos, A. P. *Science* **2001**, *292*, 2060.

Published on Web 03/12/2010

in fabricating functionalized QRs as targeted luminescence probes for fluorescence confocal, two-photon, and multiplex imaging of cancer cells as well as for traversing across the blood−brain barrier model.[5,20,21] These studies have demonstrated the advantages of functionalized QRs as long-term biocompatible probes for in vitro and in vivo imaging. A similar report by Deka et al. also emphasized on the efficiency of double-shelled QRs as biolabeling nanoprobes.[22]

As-synthesized QRs are stable in nonaqueous solutions, but to employ them in biolabeling and imaging applications, these QRs need to be transferred to the aqueous phase by means of using amphiphilic ligands. However, their photophysical behavior is affected by the use of other solvents, ligands and environment.[3,23] To maintain the photo and colloidal stability of QRs in aqueous phase, these particles need to be encapsulated within a rigid biocompatible functional matrix. To passivate the hydrophobic surface of QDs/QRs, several strategies are reported such as the use of mercapto acids as coupling reagents,[24] encapsulation within silica matrix,[3,25−27] amphipilic polymers,[24,28] or hydrophilic PEG grafted lipids.[29] Also the encapsulation of QRs/QDs into organic/inorganic hybrids attempted to passivate void on their surface.[30,31] Silica coating is an ideal choice to provide highly photostable water dispersible QRs. The silica coating of colloidal nanoparticles has been studied extensively during the past decade with a significant progress particularly in metal nanocrystals[32,33] such as Au and Ag. A wide variety of the applications of silica coating to metal, semiconductor, and inorganic colloidal particles stems from the fact that a silica layer is biocompatible and optically transparent.[34] More importantly, the silica surface can be functionalized with different reactive groups by conventional surface chemistry,[35,36] facilitating the dispersibility of coated colloids in different solvents.[37]

In this paper, we demonstrate the synthesis of biocompatible nanoparticles consisting of QRs encapsulated in a SiO_2 shell. SiO_2 coating technique is used as a nanoplatform to make other novel hybrid nanoparticle architectures for in vitro and in vivo optical imaging applications. The SiO_2 coating was introduced to the QRs through a reverse microemulsion method,[25] using Igepal CO-520 as the surfactant and cyclohexane as the "oil" solvent. The presence of the surfactant allowed the hydrophobic QRs to be encapsulated within the aqueous region of the reverse microemulsion. In our approach, a straightforward two-step process was employed to fabricate these SiO_2-coated QR nanoparticles. The first step involved the QRs preparation using the well-established method and the second step for SiO_2 encapsulation of the QRs. The water-dispersible SiO_2-coated QRs nanoparticles were systematically characterized by TEM, PL spectroscopy, and dynamic light scattering (DLS). In vitro confocal imaging was done with alveolar macrophage cells and pancreatic cancer cells Panc 1. In vivo tumor imaging was also done with nude mice. Though SiO_2-coated QDs have been previously reported and used for labeling cells, we are not aware of any reports of fabricating SiO_2-coated CdSe QRs and their applications in bioimaging.

Experimental Section

Materials and Methods. Polyoxyethylene nonylphenyl ether (Igepal CO-520), cadmium oxide, trioctylphosphine, selenium, zinc chloride, tetraoctylammonium bromide (TOAB), HPLC water, and tetraethyl orthosilicate (99.9999%) were purchased from Sigma Aldrich. Cyclohexane was obtained from Fisher. Ammonia hydroxide solution was purchased from J. T. Baker. All chemicals were used as received. All solvents (hexane, toluene, chloroform, ethanol, and acetone) were used without further purification. Microfuge membrane-filters (NANOSEP 100K OMEGA) are a product of Pall Corporation. The cell lines Panc 1 and RAW264.7 were obtained from ATCC, VA, and cultured according to instructions supplied by the vendor. Unless otherwise mentioned, all cell culture products and antibodies were obtained from Invitrogen.

Synthesis of Quantum Rods (QRs). The QRs were synthesized on the basisd of our previous work.[20] Briefly, 1.6 mmol of cadmium oxide, 3 mmol of TDPA, and 3 g of TOPO were loaded into a 100 mL, three-necked flask. Next, the reaction mixture was slowly heated under an argon atmosphere to 290−300 °C. After 10−15 min of heating, a clear homogeneous solution was obtained. The reaction mixture was maintained at 300 °C for another 5 min, and then 0.8 mL of 1 M TOP-Se was rapidly injected. The reaction was stopped after 2−3 min by removing the heating mantle. The QRs were separated from the surfactants solution by addition of ethanol and centrifugation. The reddish QR precipitate could be readily redispersed in various organic solvents (hexane, toluene, and chloroform). The synthesis method of forming a CdS/ZnS graded shell on CdSe

(20) Yong, K. T.; Qian, J.; Roy, I.; Lee, H. H.; Bergey, E. J.; Tramposch, K. M.; He, S.; Swihart, M. T.; Maitra, A.; Prasad, P. N. *Nano Lett.* **2007**, *7*, 761.
(21) Xu, G.; Yong, K. T.; Roy, I.; Mahajan, S. D.; Ding, H.; Schwartz, S. A.; Prasad, P. N. *Bioconjugate Chem.* **2008**, *19*, 1179.
(22) Deka, S.; Quarta, A.; Lupo, M. G.; Falqui, A.; Boninelli, S.; Giannini, C.; Morello, G.; Giorgi, M. D.; Lanzani, G.; Spinella, C.; Cingolani, R.; Pellegrino, T.; Manna, L. *J. Am. Chem. Soc.* **2009**, *131*, 2948.
(23) Wu, X. Y.; Liu, H. J.; Liu, J. Q.; Haley, K. N.; Treadway, J. A.; Larson, J. P.; Ge, N. F.; Peale, F.; Bruchez, M. P. *Nat. Biotechnol.* **2003**, *21*, 41.
(24) Jiang, W.; Mardyani, S.; Fischer, H.; Chan, C. W. *Chem. Mater.* **2006**, *18*, 872.
(25) Selvan, S. T.; Tan, T. T.; Ying, J. Y. *Adv. Mater.* **2005**, *17*, 1620.
(26) Yang, H.; Holloway, P. H.; Santra, S. *J. Chem. Phys.* **2004**, *121*, 7421.
(27) Tsukasa, T.; Masayuki, H.; Takahito, K.; Ken-Ichi, O.; Tamaki, S.; Bunsho, O. *J. Nanosci. Nanotechnol.* **2009**, *9*, 506.
(28) Larson, D. R.; Zipfel, W. R.; Williams, R. M.; Clark, S. W.; Bruchez, M. P.; Wise, F. W.; Webb, W. W. *Science* **2003**, *300*, 1434.
(29) Dubertret, B.; Skourides, P.; Norris, D. J.; Noireaux, V.; Brivanlou, A. H.; Libchaber, A. *Science* **2002**, *298*, 1759.
(30) Kazes, M.; Saraidarov, T.; Reisfeld, R.; Banin, U. *Adv. Mater.* **2009**, *21*, 1716.
(31) Neves, M. C.; Martins, M. A.; Soares-Santos, P. C .R.; Rauwel, P.; Ferreira, R. A. S.; Monteiro, T.; Carlos, L. D.; Trindade, T. *Nanotechnology* **2008**, *19*, 155601.
(32) Graf, C.; Vossen, D. L. J.; Imhof, A.; Blaaderen, A. v. *Langmuir* **2003**, *19*, 6693.
(33) Liz-Marzan, L. M.; Mulvaney, P. *J. Phys. Chem. B* **2003**, *107*, 7312.
(34) Velikov, K. P.; Blaaderen, A. v. *Langmuir* **2001**, *17*, 4779.
(35) Santra, S.; Zhang, P.; Wang, K. M.; Tapec, R.; Tan, W. H. *Anal. Chem.* **2001**, *73*, 4988.
(36) Rogach, A. L.; Nagesha, D.; Ostrander, J. W.; Giersig, M.; Kotov, N. A. *Chem. Mater.* **2000**, *12*, 2676.
(37) Lu, Y.; Yin, Y. D.; Li, Z. Y.; Xia, Y. A. *Nano Lett.* **2002**, *2*, 785.

quantum rod was adapted from that presented by Manna et al.[38,39] CdSe quantum rods solution was prepared in advanced by dissolving ~0.2 g of CdSe QRs in ~5 mL of toluene. Separately, 2 mmol of cadmium oxide, 4 mmol of zinc acetate, and 5 g of TOPO were dissolved in 10 mL of oleic acid. The reaction mixture was heated to 170 °C for ~30 min under an argon flow and the CdSe nanorods solution was injected slowly under stirring into the hot reaction mixture. The reaction mixture was held at 170 °C, with a needle outlet that allowed the toluene to evaporate. After ~10 min of heating, the needle was removed, and then the reaction temperature was raised to 200−210 °C. Upon reaching the desire temperature, a 2 mL of TOP-S was added dropwise into the reaction mixture. The reaction mixture was then held at ~210 °C for 10−15 min and an aliquot was then removed via syringe and injected into a large volume of toluene at room temperature, thereby quenching any further growth of the QRs. The QRs were separated from the toluene solution by addition of ethanol and centrifugation.

Synthesis of QRs Encapsulated in Silica Shell (SiO_2/QRs). The synthesis procedures for the SiO_2 coated nanoparticles were adapted from previous reports with several modifications.[25] Briefly, 60 μL of ammonia hydroxide, 0.53 g of Igepal CO-520, and 150 μL of cyclohexane solution containing 2 mg/mL CdSe/CdS/ZnS QRs were mixed with 10 mL of cyclohexane. The mixture was vigorously stirred for 30 min. After 30 min of stirring, 0.5 mL of cyclohexane solution containing 0.056 g/mL TEOS precursor was injected into the mixture and the mixture was stirred for additional 20 h at room temperature. The particles were extracted from the microemulsion by adding 1 mL of ethanol and centrifugation at 11 000 rpm for 30 min. The obtained pellet was washed 2 times with ethanol and finally the silica-coated QRs were dispersed in water and stored at 4 °C.

Cell Staining Studies. For in vitro imaging, with silica-coated QRs, the human pancreatic cancer cell line Panc 1 as well as macrophages RAW264.7 were cultured in Dulbecco minimum essential media (DMEM) with 10% fetal bovine serum (FBS), 1% penicillin, and 1% amphotericin B. The day before nanoparticles treatment, cells were seeded in 35 mm culture dishes. On the treatment day, the cells, at a confluency of 70−80% in serum-supplemented media, were treated with the nanoparticles at a specific concentration (100 μL/ml media; 2.5 μg/mL nanoparticles concentration) for 24 h at 37 °C.

Cell Viability Assay. The Panc 1 cells were dispensed into a 96-well flat-bottom microtiter plate (~10,000 cells/well) and allowed to attach overnight using the DMEM medium with 10% FBS. The MTS assay was carried out as per manufacturer's instructions (PROMEGA). It is based on the absorbance of formazan (produced by the cleavage of MTS by dehydrogenases in living cells), the amount of which is directly proportional to the number of live cells. In brief, after 24 and 48 h treatment with the SiO_2-coated QRs, media was changed and 150 μL of MTS reagent was added to each well and well-mixed. The absorbance of the mixtures at 490 nm was measured. The cell viability was calculated as the ratio of the absorbance of the sample well to that of the control well and expressed as a percentage. Tests were performed in quadruplicate. Each point represents the mean ± SD (bars) of replicates from one representative experiment.

UV−Visible Absorbance. The absorption spectra were collected using a Shimadzu model 3101PC UV−vis−NIR scanning spectrophotometer over a wavelength range from 300 to 800 nm. The samples were measured against water as reference. All samples were used as prepared and loaded into a quartz cell for measurements.

Photoluminescence (PL) Spectroscopy. The emission spectra were collected using a Fluorolog-3 Spectrofluorometer (Jobin Yvon). All the samples were dispersed in water and loaded into a quartz cell for measurements.

Transmission Electron Microscopy (TEM). Transmission electron microscopy (TEM) images were obtained using a JEOL model JEM- 100CX microscope at an acceleration voltage of 80 kV. The specimens were prepared by drop casting the sample dispersion onto an amorphous carbon coated 300 mesh copper grid, which was placed on a filter paper to absorb the excess solvent.

Confocal Microscopy. Confocal Microscopy images were obtained using a Leica TCS SP2 AOBS spectral confocal microscope (Leica Microsystems Semiconductor GmbH, Wetzler, Germany) with laser excitation at 442 nm. All images were taken under exact same conditions of laser power, aperture, gain, offset, scanning speed, and scanning area.

In vivo Imaging of Silica-Coated QRs. In vivo optical imaging of the mice body was done using a Maestro GNIR FLEX fluorescence imaging system (Cambridge Research & Instrumentation, CRi). Balb C mice were used for intratumoral injection which was xenografted on the shoulder of the mouse. Two-hundred microliters of 2 mg/mL silica-coated QRs in water with 5% glucose was injected. Imaging was done immediately after the injection. The silica coated QRs were excited at 488 nm by the xenon lamp. The emission filter 600LP was used to cut off excitation light.

Wavelength-resolved spectral imaging (for both in vitro and in vivo) was carried out using a spectral imaging system (CRI) comprising an optical head, an optical coupler and a cooled, scientific-grade monochrome CCD camera, along with the image acquisition and analysis software. The tunable filter was automatically stepped in 10 nm increments from 580 to 950 nm, while the camera captured images at each wavelength with constant exposure. The overall acquisition time was about 10 s. The 13 resulting TIFF images were loaded into a single data structure in the memory, forming a spectral stack with a spectrum at every pixel. With spectral imaging software, small but meaningful spectral differences could be rapidly detected and analyzed. The autofluorescence spectra and the SiO_2/QRs spectra were manually selected from the spectral image using the computer mouse to select appropriate regions. Spectral unmixing algorithms (available from CRI) were applied to create the unmixed images of "pure" autofluorescence and "pure" nanoparticle signal. When appropriately generated, the autofluorescence image should be uniform in intensity, regardless of the presence or absence of the silica coated QRs signal. The identification of valid spectra for unmixing purposes need only be done initially, as the spectra can be saved in spectral libraries and reused on additional spectral stacks.

Results and Discussion

Synthesis and Characterization of Silica-Coated QRs. The formation of silica layer on the surface of CdSe/CdS/ZnS QRs has been carried out using the reverse microemulsion approach. The interaction between hydrophilic groups of the surfactant layers of QRs and Igepal CO-520 allows the hydrophobic QRs to be encapsulated within the aqueous core of the reverse microemulsion droplets. The aqueous dispersibility of the silica coated QRs itself

(38) Manna, L.; Scher, E. C.; Alivisatos, A. P. *J. Am. Chem. Soc.* **2000**, *122*, 12700.
(39) Manna, L.; Scher, E. C.; Li, L.-S.; Alivisatos, A. P. *J. Am. Chem. Soc.* **2002**, *124*, 7136.

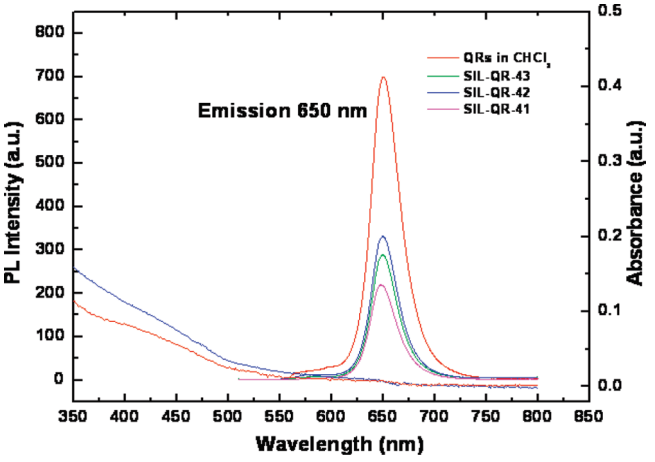

Figure 1. Absorption and PL spectra of different formulations of SiO_2-coated CdSe/CdS/ZnS QRs.

indicates the formation of a silica shell on the surface of the QR. The negative charge (zeta potential = −24.5 mV) of the silica coated QRs indicates the presence of hydrophilic hydroxyl (Si−OH) on the silica shell which renders the QRs water dispersible.[37] In contrast, the uncoated CdSe/CdS/ZnS QRs, when dispersed in water, precipitated within ~30 min. We have also varied the thickness of the silica shell on the QRs surface and studied the effect of shell thickness on aqueous stability and shelf life of the final formulations. We have observed that for shell thickness above 25 nm, the samples (SILQR43) were less stable and aggregated over a period of 7−8 days, which can be attributed to the agglomeration of the silica shell of individual silica coated QRs, whereas for samples with shell thickness less than 3 nm remained well-suspended in water, with no aggregation for more than a month. A similar stability has been observed for the nanoparticles suspension dispersed in PBS (1X, pH 7.4) as well as 5% glucose solution for maintaining the isotonicity with the physiological conditions.

Figure 1 shows the absorption and photoluminescence (PL) spectra of the silica-coated QR dispersion in water. The absorption spectra showed the typical excitonic band for CdSe/CdS/ZnS QRs. The PL spectra showed the emission band at 650 nm for both silica-coated QRs aqueous dispersion and uncoated QRs in chloroform. It can also be observed from the figure that there is no considerable shift in the PL emission band. However, with the change in silica shell thickness, a blue shift of 3 nm was observed for the sample with minimum silica shell thickness (SILQR41: emission λ_{max} 647 nm). It can be seen that although the PL intensity of the silica-coated QRs was slightly decreased during the preparation, the aqueous dispersion of silica-coated QRs still showed very good PL intensity, with a quantum yield close to 7% that is in good correlation with similar formulation reported by other groups.[40,41] The decrease in PL intensity can be attributed to the surface desorption of QR surfactant with Igepal and the alkaline pH used for TEOS polycondensation.[25,42] Also, it was observed that increasing the thickness of the silica shell enhances the photostability of the SiO_2/QRs nanoparticles with respect to fluorescence intensity, which also indicates a diffusional constraint for molecular oxygen to interact with the QRs encapsulated inside the silica matrix.[40]

Figure 2 shows the representative high-resolution TEM images of the aqueous dispersion of the silica coated QRs, as compared to the uncoated QRs in chloroform. The silica shell can be differentiated easily by the contrast between the light silica shell and darker CdSe/CdS/ZnS QRs.

All the samples prepared were monodispersed with shape depending on the shell thickness of silica on QRs surface, which varied from spherical to oblong with decreasing the silica shell thickness. The silica shell thickness can be varied by manipulating the TEOS concentration (see the Supporting Information). As can be observed from the figure, a single QR was encapsulated within each silica shell. The TEM image (Figure 2c) of the uncoated CdSe/CdS/ZnS QRs showed a size of 5 nm width to 24 nm in length. A comparison between Figure 2a, b and 2c showed a clear growth of the silica shell on the of QRs surface. Figure 3 shows the comparative high-resolution TEM images of the QRs coated with varying thickness of the silica shell. We have prepared three different formulations of QRs coated with different thickness of the silica shell (see Table 1). The silica shell tuning was done from 3 to 25 nm. Images a and d in Figure 3 (HRTEM) show the QRs coated with silica shell with the shell thickness of ~34 nm along the length, whereas the overall size of the nanoparticles was found to be 80 ± 2 nm (SILQR43). The morphology of the nanoparticles is almost spherical as can be visualized from the figure. Images b and e in Figure 3 (SILQR42) show the nanoparticles with a shell thickness of ~10 nm, which resulted in an oblong morphology of the nanoparticles, whereas the minimum shell thickness that was possible to coat on to the surface of QRs was ~3 nm, with the overall size of the nanoparticles being 27 ± 3 nm (Figure 3c,f: SILQR41).

It is quite evident that the concentration ratio between the TEOS and QRs plays an important role in determining the silica shell thickness as well as the number of cores present in the silica nanoparticles. When higher QRs concentration of 7.5 mmol was used, irregular-shaped nanoparticles with multiple cores were obtained, whereas at a concentration of 2 mmol, the particles obtained were with single QR encapsulated in each SiO_2 shell. Figure 3g−i shows the corresponding DLS spectrum of the all three formulations. The DLS data showed a good correlation with the TEM.

Though many groups have developed novel strategies in fabricating silica-coated nanocrystals such as quantum dots, magnetic nanoparticles, and metal nanoparticles,

(40) Yang, Y.; Gao, M. *Adv. Mater.* **2005**, *17*, 2354.
(41) Chan, Y.; Zimmer, J. P.; Stroh, M.; Steckel, J. S.; Jain, R. K.; Bawendi, M. G. *Adv. Mater.* **2004**, *16*, 2092.
(42) Ando, M.; Li, C.; Yang, P.; Murase, N. *J. Biomed. Biotechnol.* **2007**, *2007*, 52971.

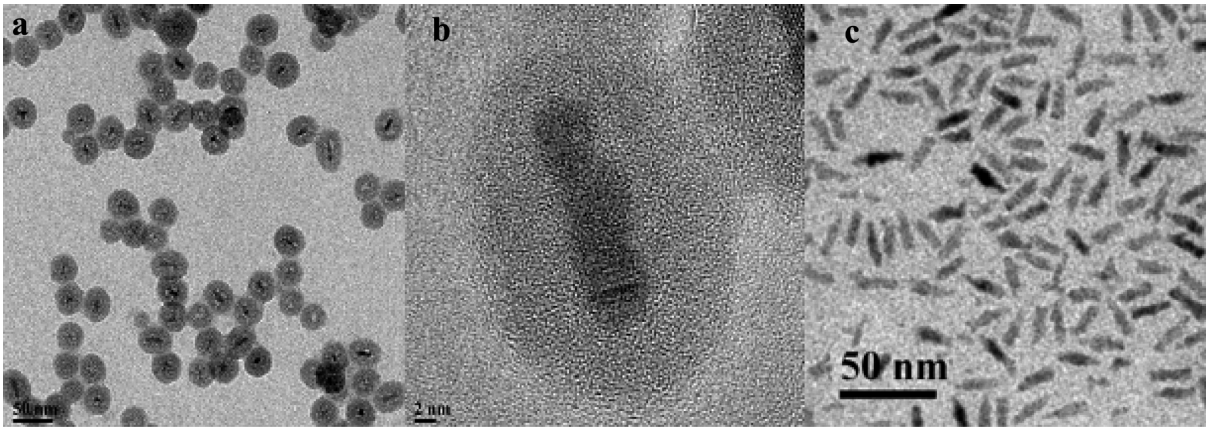

Figure 2. Representative TEM images of (a) SiO_2-coated QRs, (b) high-resolution image of a single nanoparticle in the aqueous medium, and (c) CdSe/CdS/ZnS QRs in chloroform.

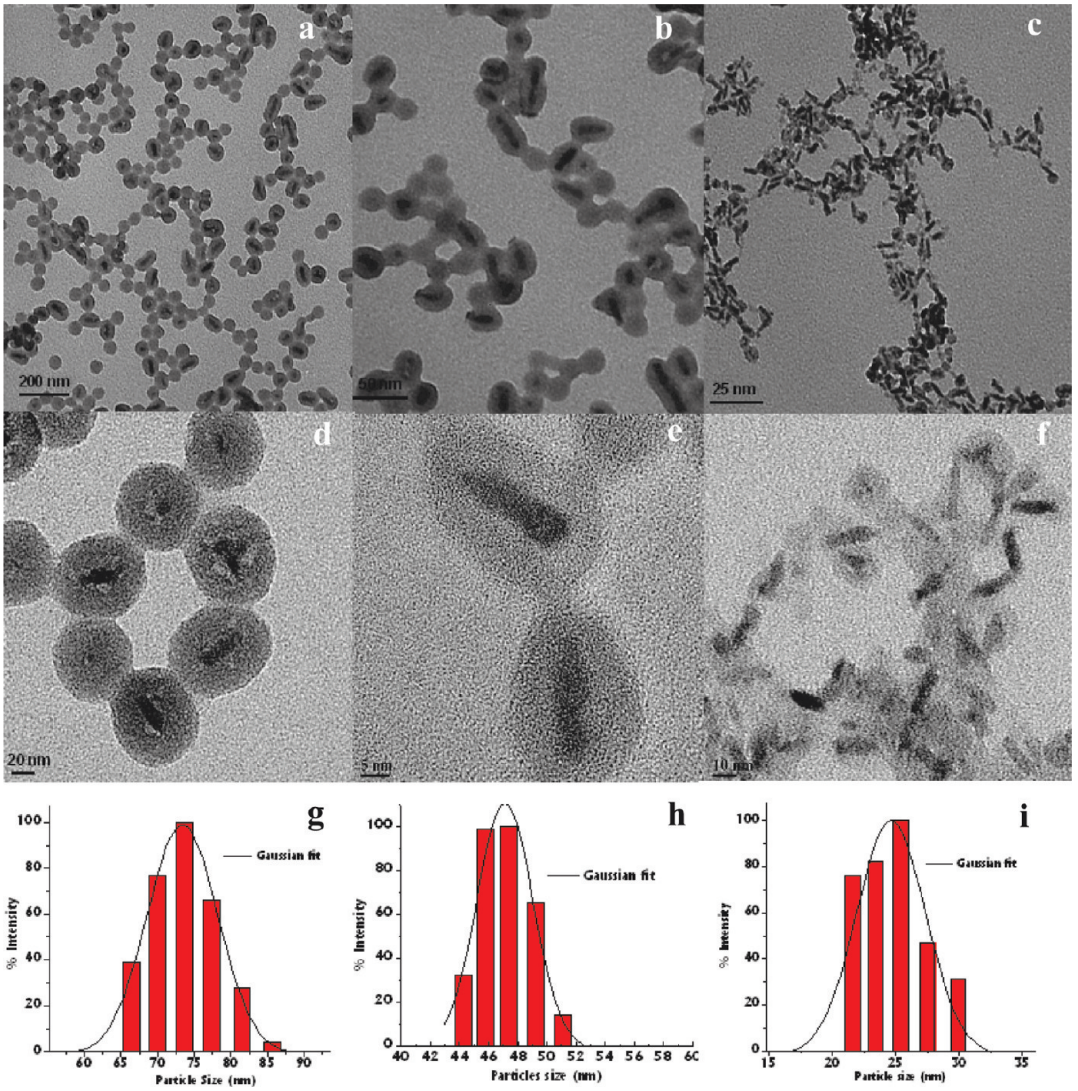

Figure 3. Size distribution studies of SiO_2-coated QRs: (a−c) different silica shell thickness TEM images, (d−f) high-resolution TEM images of the corresponding nanoparticles, and (g−i) DLS size distribution.

very few studies are available in the literature in using these nanoparticles for biological applications. These may be due to the challenges in making them colloidally stable in aqueous phase with maintaining the fluorescence properties. Also, many of the protocols in synthesizing silica coated nanoparticles contain surfactants that promote a toxicity effects in the cellular environment. Thus, there is a need to optimize the current recipes for making low-toxicity, biocompatible, and monodipersed silica-coated nanoparticles for targeted bioimaging.

Table 1. Size Distribution of Different Formulations of SiO_2-Coated QRs

	particle size (nm)		
sample	SiO_2 shell thickness	DLS	TEM
SILQR 41	3.0	27 ± 3	12 ± 1 width/26 ± 2 length
SILQR 42	10.0	47 ± 3	24 ± 3 width/42 ± 1 length
SILQR 43	21.3 along width/34.0 along length	80 ± 2	68 ± 3

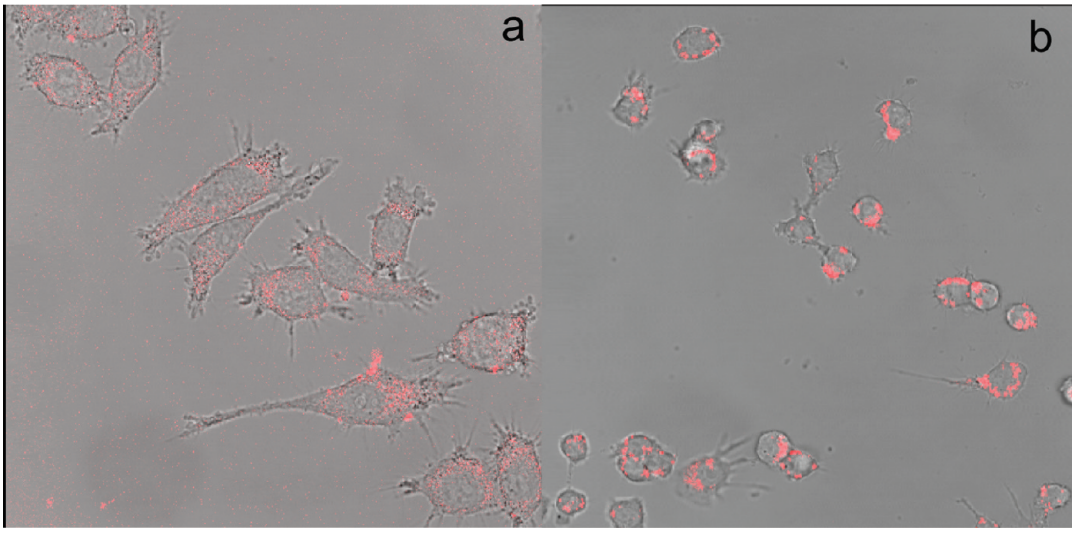

Figure 4. Confocal Images of (a) Panc 1 and (b) RAW cell line treated with aqueous dispersion of SiO_2-coated CdSe/CdS/ZnS QRs. Images were acquired after 24 h incubation of nanoparticles.

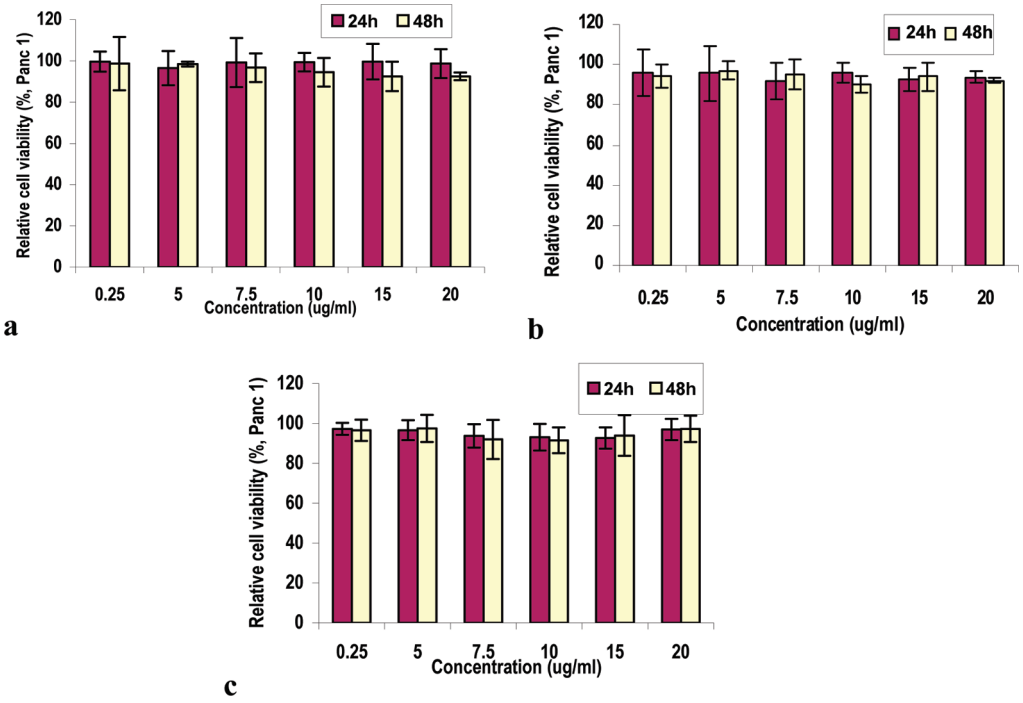

Figure 5. Cytotoxicity studies done by the MTS assay method for the three different formulations of SiO_2-coated QRs: (a) SILQR 41, (b) SILQR 42, and (c) SILQR 43.

To demonstrate that the SiO_2-coated QR nanoparticles are capable for bioimaging, the SiO_2/QRs particles are used to label two different cell lines, the pancreatic cancer cell line Panc-1 as well as the RAW macrophage cells. Fluorescence confocal images of live cells incubated with 2.5 μg/mL SiO_2 coated QRs nanoparticles for 24 h are shown in Figure 4. It is quite evident from the confocal image that a large number of nanoparticles were internalized and accumulated in the cytoplasm by phagocytosis. Notably, no morphological damage was observed for both the cell lines, indicating low cytotoxicity of these nanoparticles. This demonstrated that the SiO_2-coated

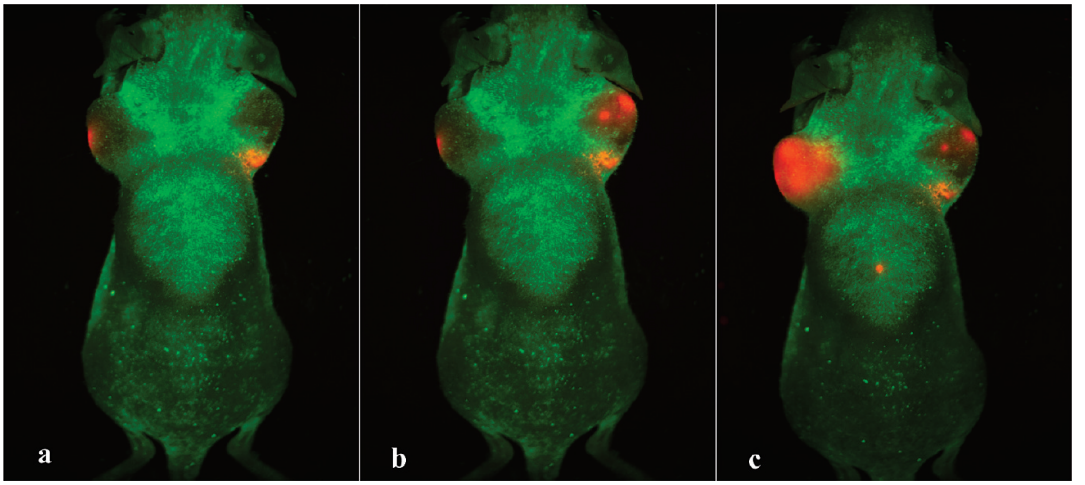

Figure 6. Whole body images of subcutaneously xenografted tumored mice intratumoraly injected with SILQR 42 at (a) 1 (b) 5, and (c) 10 min post-injection.

QRs nanoparticles were biocompatible, stable, and suitable for in vitro cell labeling, cell tracking, and other bioimaging applications.

To estimate the cytotoixicity of the SiO_2 coated QRs nanoparticles, we have carried out a series of MTS assay study with Panc 1 cell line for all the three formulations of variable SiO_2 shell thickness. MTS assay was performed over a period of 24 to 48 h with a variable nanoparticles dose over a range of 0.25−20 μg/mL. The confocal images of the cells treated with varying concentrations of the nanoparticles showed a higher uptake of the nanoparticles with the increase in concentration (see the Supporting Information, Figure S2). Figure 5 shows the in vitro cytotoxicity effects of SiO_2/QRs particles on the Panc 1 and the RAW cell lines. One can observe that both cell lines retained more than 80% viability even in the presence of a high SiO_2/QR nanoparticle loading of 20 μg/mL for 24 and 48 h.

The low in vitro cytotoixicity of SiO_2-coated QRs could be attributed to the fact that a thick layer of ZnS and an outer layer of biocompatible silica prevents the breakdown of the CdSe core, which is in correlation with work done by other groups.[25] Also, the hindered diffusion of the Cd^{2+} released upon the photo-oxidation of the CdSe/CdS/ZnS QRs through the silica shell can consequently reduce the cytotoixicity of these nanoparticles in biological applications.[36]

The efficient labeling of the cells in vitro as well as low cytotoxicity even at high nanoparticles dosage prompted us to use these core−shell-based nanoparticles for in vivo imaging. To investigate the applicability of silica-coated QRs for tumor imaging, 50 μL of the QRs coated with silica (QRSIL42) was injected intratumorly into the mice, bearing a panc 1 subcutaneously xenografted tumor. As can be seen from Figure 6, strong luminescences signal from the SiO_2-coated QRs can be acquired within 10 min. The green color shows the scattered excitation light. The bright red color showed the typical 650 nm emission band of the QRs. It was also observed that over a small period of 10 min, the nanoparticles spread around the tumor region and remained localized there. Further studies involving a systemic administration of the nanoparticles via the intravenous route and their subsequent biodistribution studies are required to show the in vivo toxicity and clearance from the animal body.

Conclusions

Highly water dispersible, colloidally stable ,and fluorescent silica-coated CdSe/CdS/ZnS QRs were successfully synthesized. The silica shell thickness can be varied from 2 to 25 nm. TEM and DLS studies showed a good correlation of the size of the nanoparticles. It was observed that increasing the shell thickness resulted in an increase in photoluminescence, which indicated the stabilization of the QRs by the silica shell. Different cell lines, labeled with silica-coated QRs, showed robust uptake and good fluorescence from the nanoparticles with low cytoxicity. The fluorescence from the tumor with no visible toxicity to the experimental animal showed the potential of these silica-coated QRs in various biological labeling applications, including whole body in vivo optical imaging involving tumor targeting and diagnosis.

Acknowledgment. This study was supported by NIH Grants CA119397 and CA104492 and the John R. Oishei Foundation. Lisa A. Vathy is acknowledged for her technical help.

Supporting Information Available: Description of the synthetic scheme, figure showing dependence of silica shell thickness on TEOS concentration. This material is available free of charge via the Internet at http://pubs.acs.org.